Turbulent Fluxes Over Arctic Sea Ice: Measurements, Interactions, and Comparisons to Models

P. Ola G. Persson[1, 2], Andrey Grachev[1, 2], Chris Fairall[2], Ian M. Brooks[3], Cathryn Birch[3], Amy Solomon[1, 2], and Cassie Wheeler[4]

[1]Cooperative Institute for Research in Environmental Sciences, Univ. of Colorado, Boulder, CO USA
[2]NOAA Earth System Research Laboratory, Physical Sciences Division, 325 Broadway, Boulder, CO
[3]Inst. for Atmospheric Science, University of Leeds, Leeds, United Kingdom
[4]Dept. of Atmospheric and Oceanic Sciences, Univ. of Colorado, Boulder, CO USA

CIRES/NOAA/ESRL/PSD3 Observational Data Sets

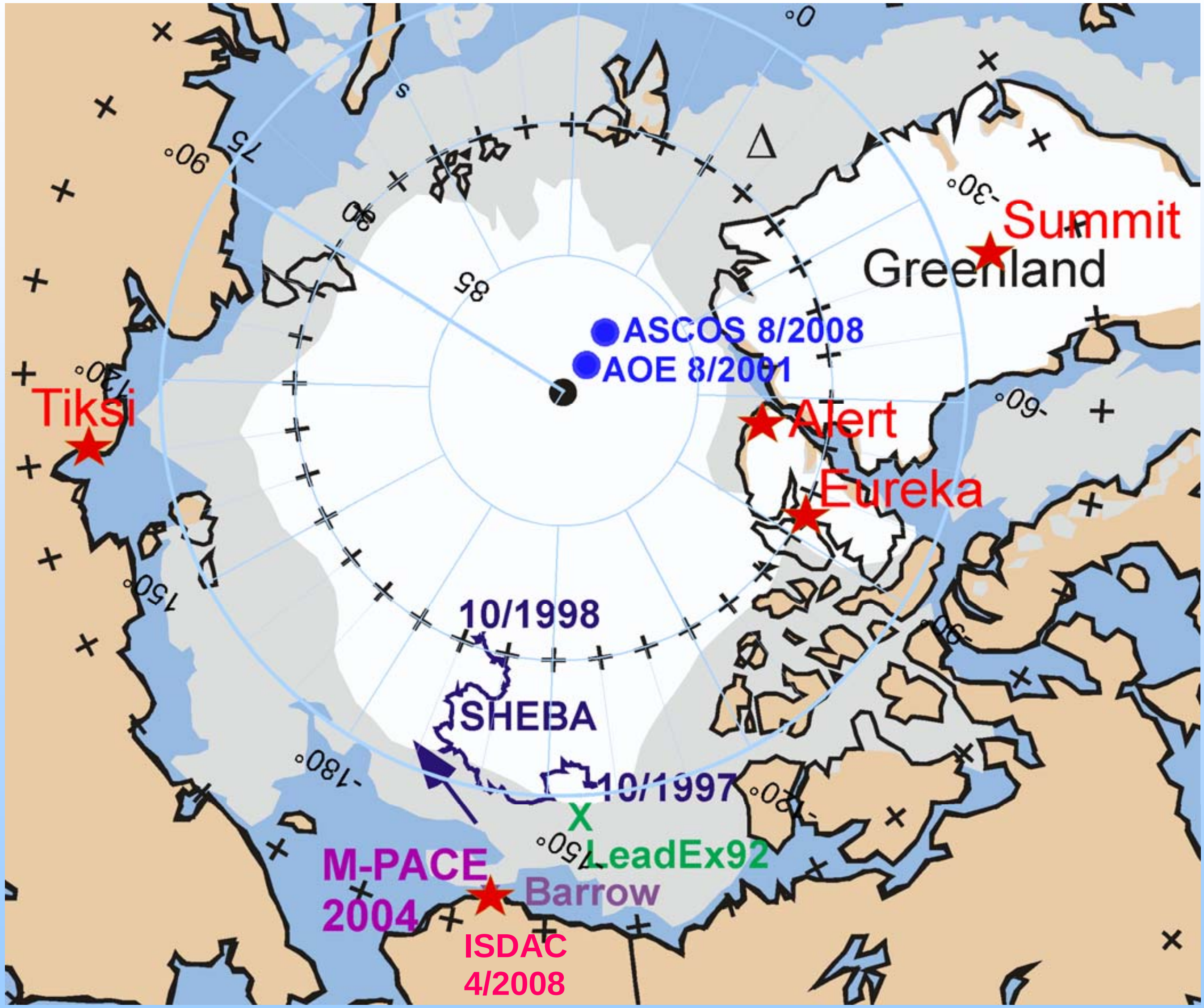

SHEBA Site

Surface Heat Budget of the Arctic Ocean Experiment (SHEBA)

- **The main SHEBA ice camp was deployed on the ice in the vicinity of the Canadian Coast Guard ice breaker *Des Groseilliers*, which was frozen into the Arctic ice pack north of Alaska from October 1997 to October 1998.**
- **During this period, the ice breaker drifted more than 1400 km in the Beaufort and Chukchi Seas, with coordinates varying from approximately 74° N and 144° W to 81° N and 166° W.**

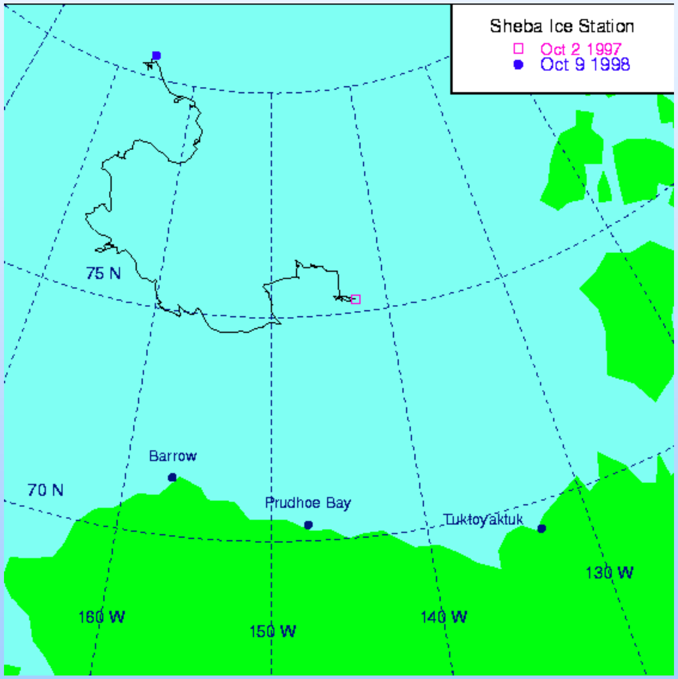

The SHEBA ice station drift from October 2, 1997 until October 9, 1998.

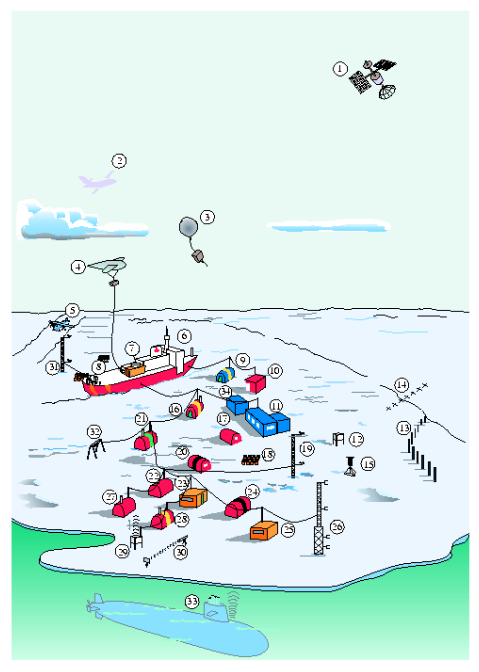

The SHEBA camp

The *Des Groseilliers* and C-130

ASFG Instrumentation

- The Atmospheric Surface Flux Group (ASFG) deployed a 20-m main micrometeorological tower, two short masts, and several other instruments on the surface located 280 – 350 m from the *Des Groseilliers* at the far edge of the main ice camp.
- Turbulent and mean meteorological data were collected at five levels, nominally 2.2, 3.2, 5.1, 8.9, and 18.2 m (or 14 m during most of the winter).
- Each level had a Väisälä HMP-235 temperature/relative humidity probe (T/RH) and identical ATI three-axis sonic anemometers/thermometers (accuracy: wind speed ±0.03 m/sec; sonic temperature ±0.1°C).
- An Ophir fast infrared hygrometer was mounted on a 3-m boom at an intermediate level just below level 4 (8.1 m above ice).

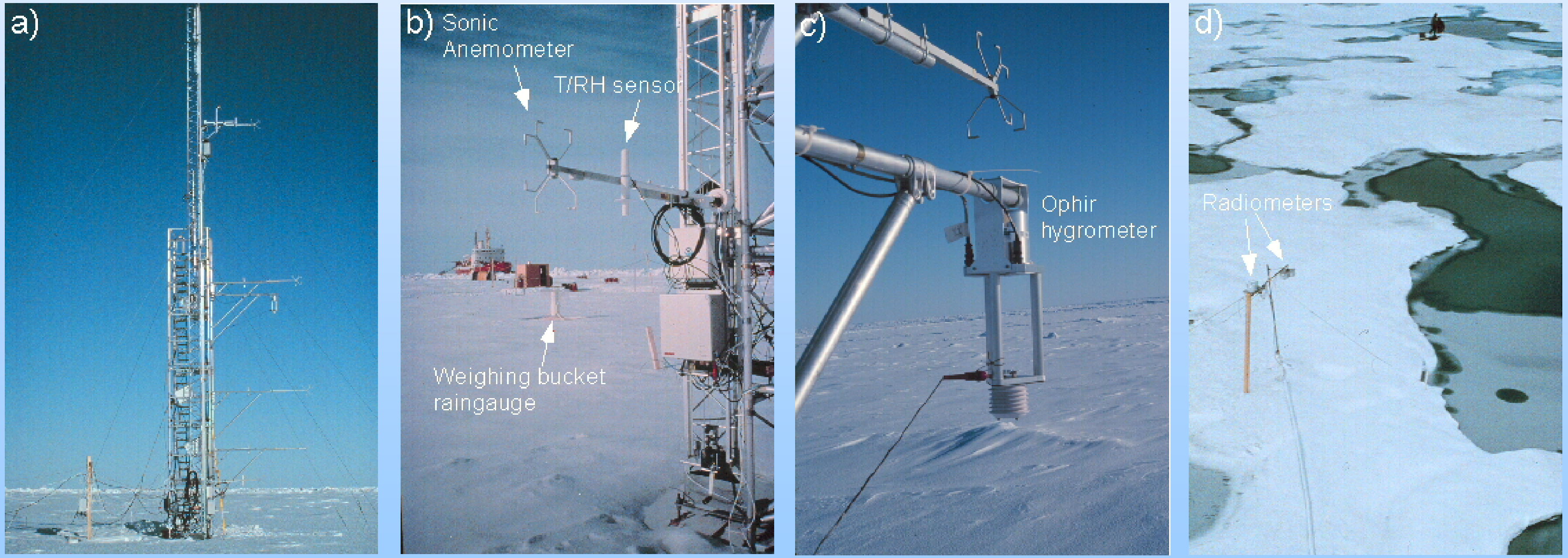

SHEBA Turbulent and Radiative Fluxes

only year-round turbulent flux observations over sea ice

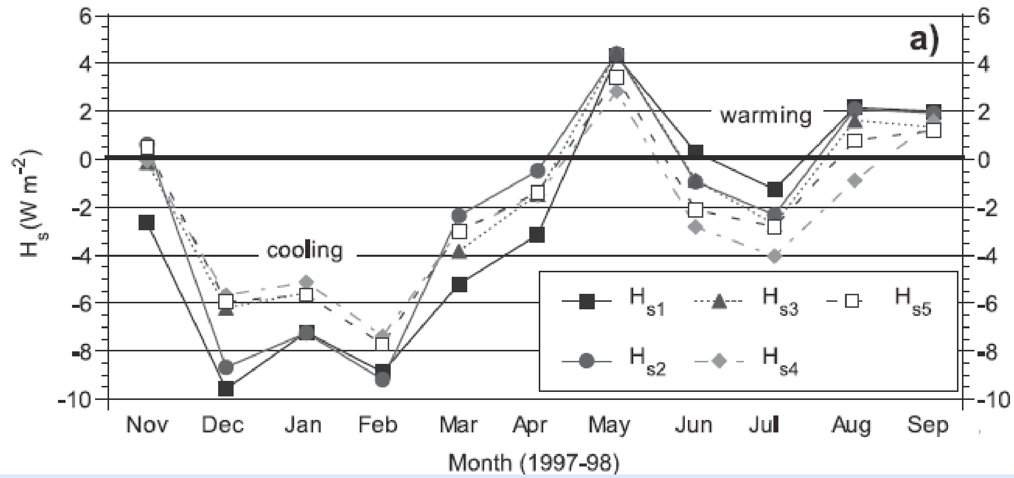

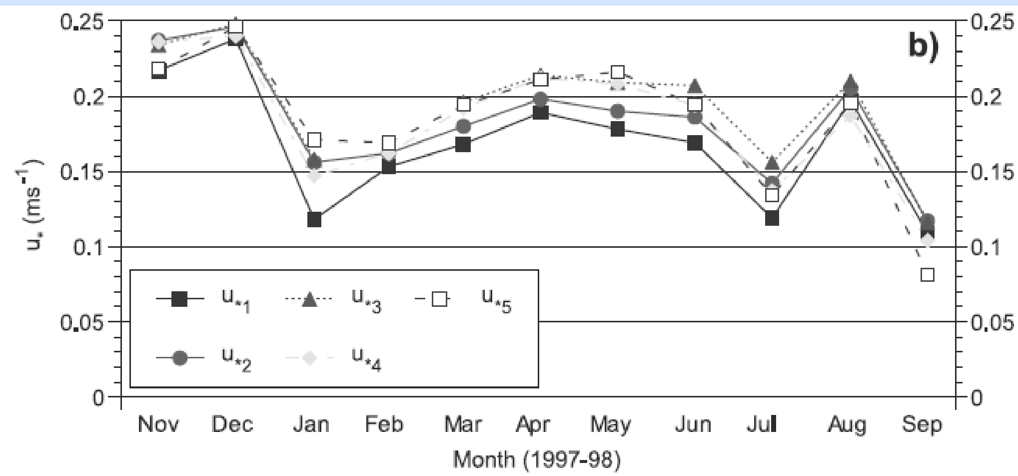

Monthly-mean values of (a) sensible heat flux (H_s) and (b) u_* for concurrent data at the five tower levels. Note that the warming/cooling refers to the air, not the surface (Persson et al. 2002, *JGR*, **107**(C10)).

1) H_s negative in winter and summer, positive late spring & early fall

2) H_s vertical flux divergence implies cooling in winter and warming in summer

3) consistent with a) wintertime cooling of PBL due to radiative cooling of surface and b) summertime warm air advection over melting surface heating PBL

-increase in u_* with height implies surface near tower smoother than that further away (z_0 = 3.1 - 6.0 x 10^{-4} m)

SHEBA Turbulent Fluxes – Diurnal Cycle

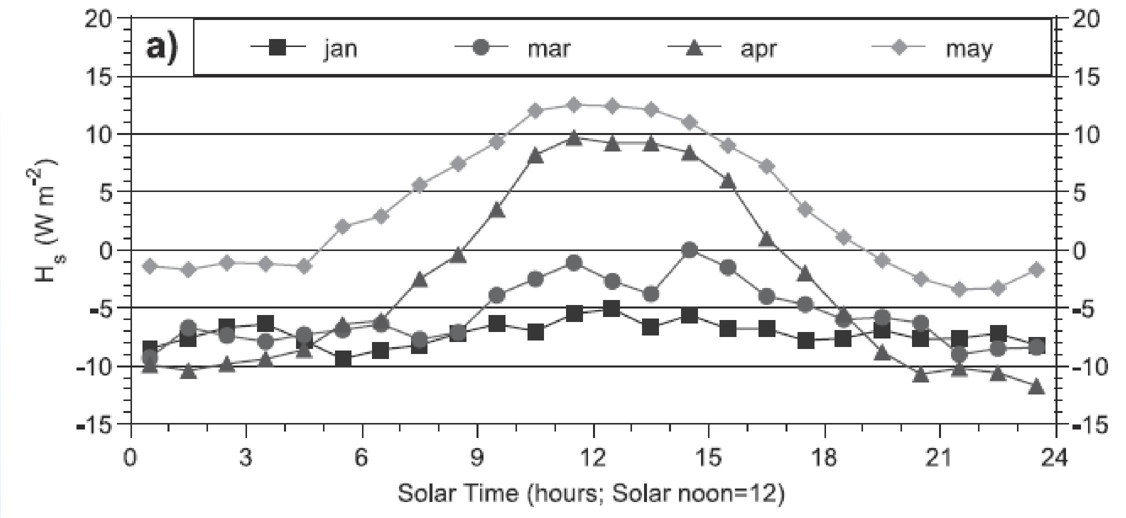

- when T_s is free to vary and solar radiation is present, a significant diurnal cycle occurs

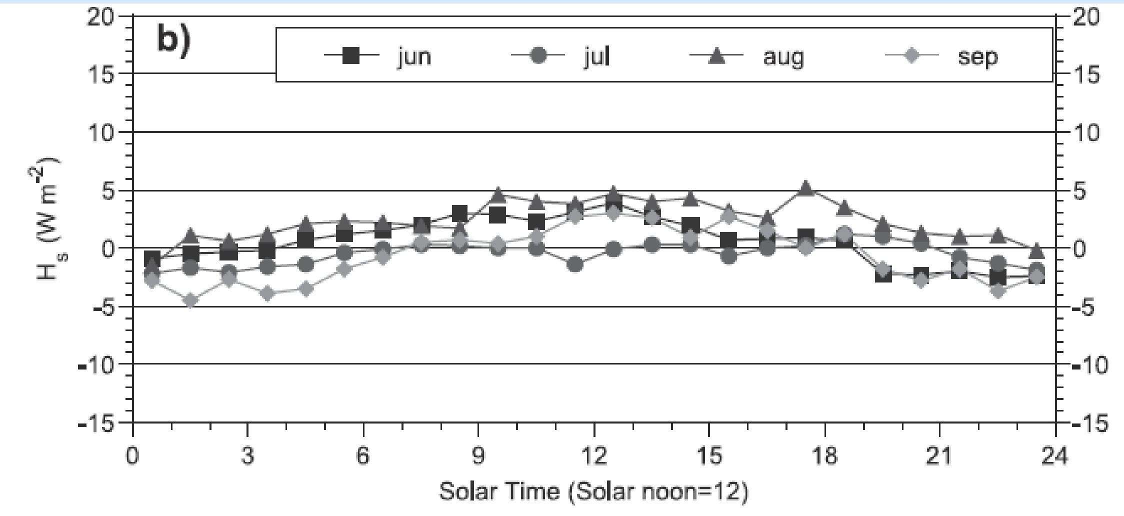

- when T_s is fixed due to melting, diurnal cycle is damped

The diurnal amplitudes of temperature from level 1 (1.9–3.0 m) for (a) January, March, April and May, and (b) June, July, August, and September. Each hourly value is the monthly mean of the daily diurnal perturbation temperature for that hour (i.e., the daily mean was subtracted) (Persson et al. 2002, *JGR*, **107**(C10)).

Stable Boundary Layer Regimes

According to the SHEBA data, stratification and the Earth's rotation control the SBL over a flat rough surface. Different SBL regimes are described in terms of the Monin-Obukhov stability parameter (*z/L*), the Ekman number (Ek) that quantifies the influence of the Earth's rotation, and the bulk Richardson number (Ri_B) that determines the intensity of the turbulence. These three non-dimensional parameters govern four major regimes (see Figure).

Figure shows a schematic diagram of the SBL scaling regimes as functions of the stability and height. Here $z_1 \approx 2$ m (level 1), $Ek_{cr} \approx 1$, $Ri_B \approx 0.2$. Dividing lines between the scaling regions are sketched.

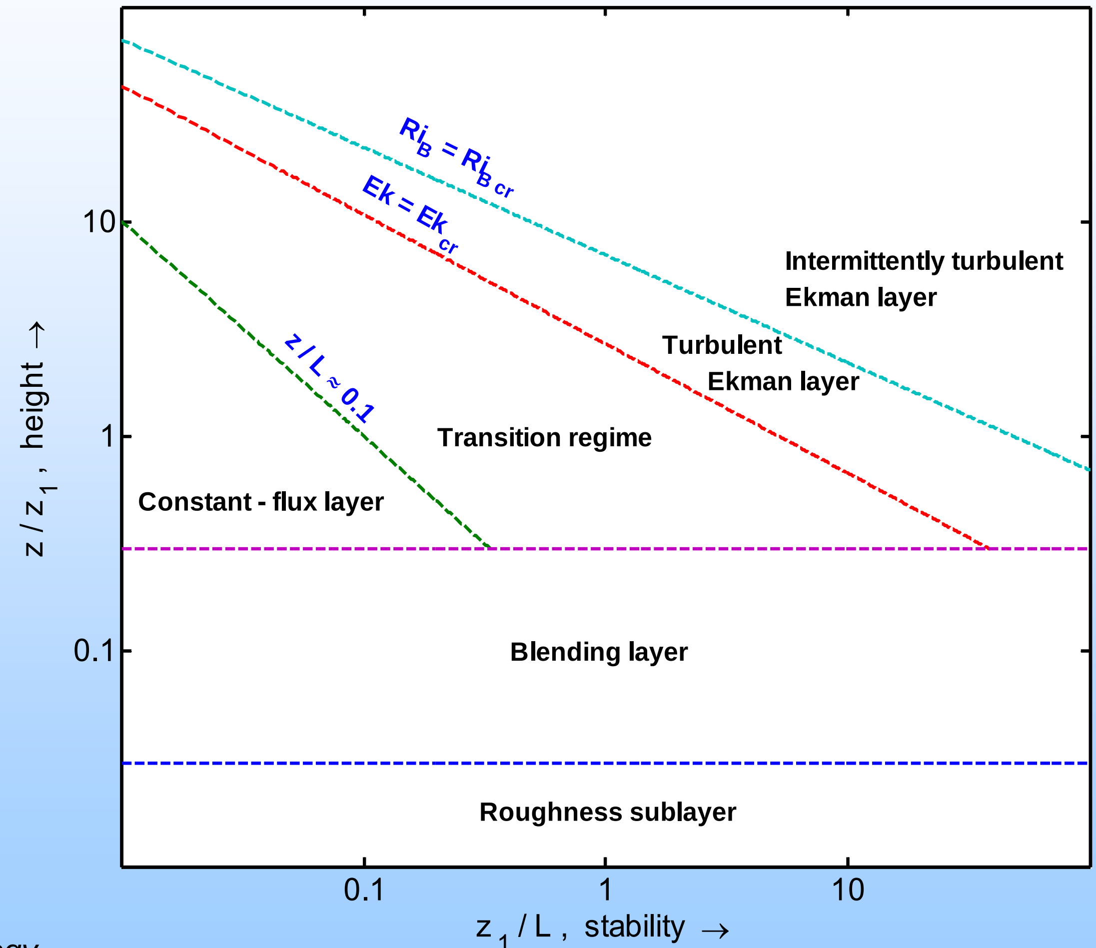

Grachev et al. (2005), *Boundary-Layer Meteorology*, **116**(2), 201-235.

Turbulence Decay in the Stable ABL

Momentum and sensible heat fluxes near the critical Richardson number

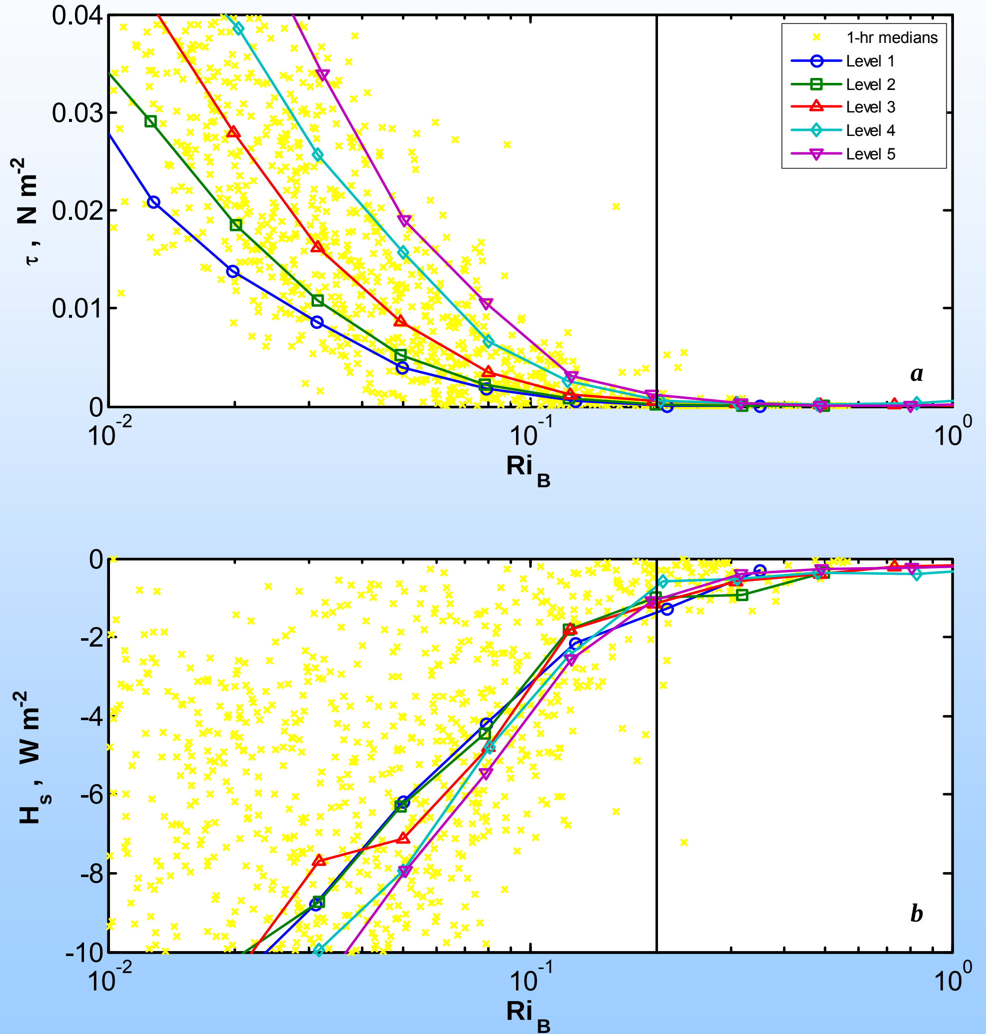

Typical Turbulent Cospectra

for weakly and moderate stable (left) and very stable (right) conditions

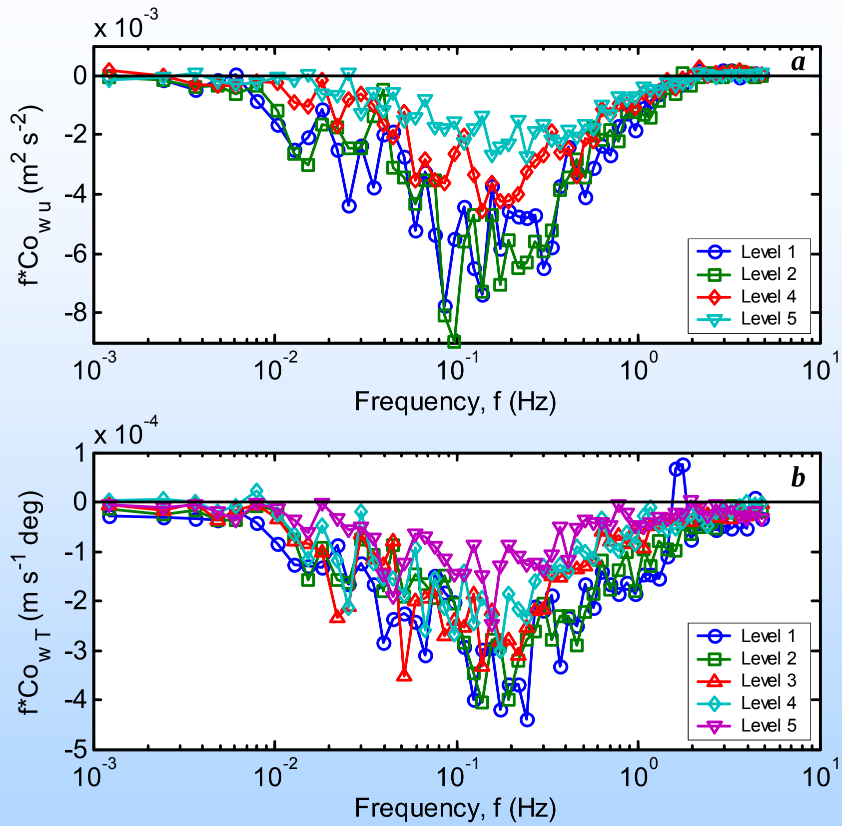

Typical (*a*) stress cospectra (1998 JD 45.4167), and cospectra of the sonic temperature flux (1997 JD 324.5833) for weakly and moderate stable conditions . In (*a*) u_* decreases with increasing height from 0.134 to 0.08 m/s. Stability parameter increases with increasing height from 0.128 to 1.893. In (*b*) downward sensible heat flux decreases with increasing height from -1.66 to -0.64 W/m^2 (level 1 to level 5). Stability parameter increases with increasing height from 0.096 to 0.533.

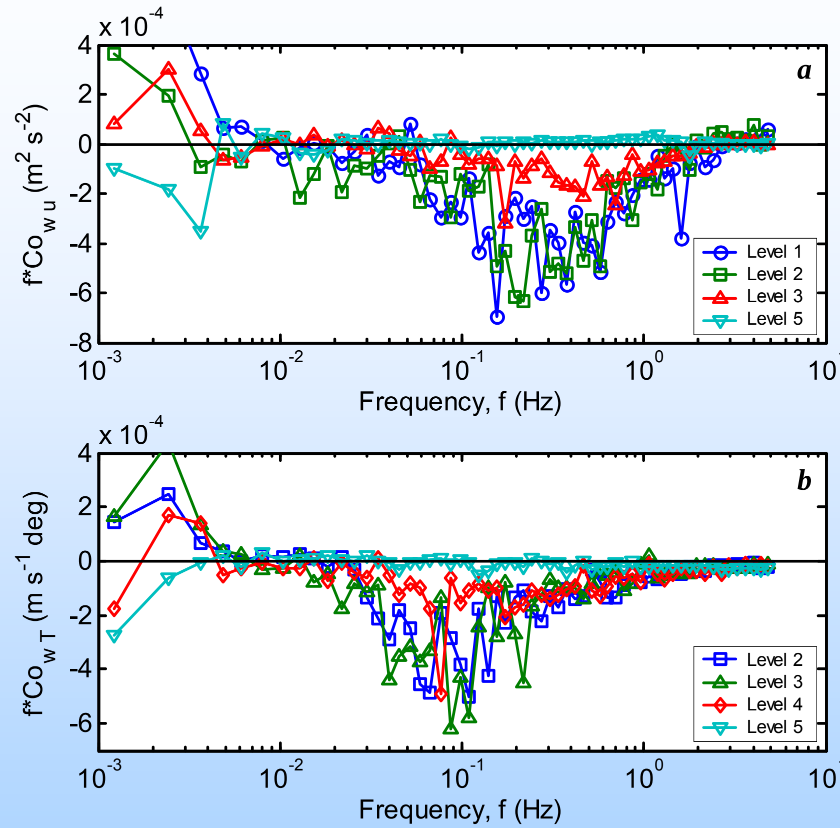

Typical cospectra of (*a*) the momentum flux (JD 355.00, 21 Dec., 1997), and (*b*) the sonic temperature flux (JD 507.75, 22 May, 1998) in the very stable regime. In (*a*) the stability parameter is 3 (level 2) and 10.5 (level 3). In (*b*) the stability parameters increase with increasing height: 1.41, 2.05, 6.34, 8.13 (levels 2–5).

Typical Turbulent Spectra

for weakly and moderate stable (left) and very stable (right) conditions

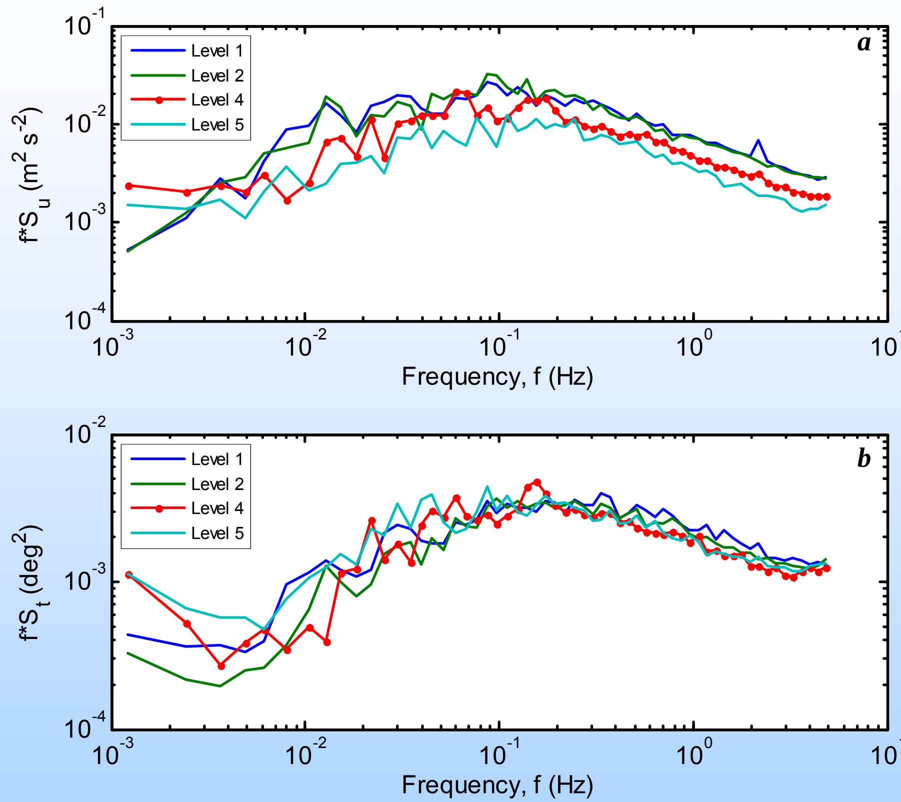

Typical raw spectra of (*a*) the longitudinal wind component and (*b*) the sonic temperature at four levels (level 3 is missing) for weakly and moderate stable conditions during 14 February 1998 UTC (1998 YD 45.4167). Stability parameter increases with increasing height from 0.128 to 1.893, (levels 1, 2, 4, and 5). The bulk Richardson number also increases with increasing height from 0.0120 to 0.0734 but it is still below its critical value 0.2.

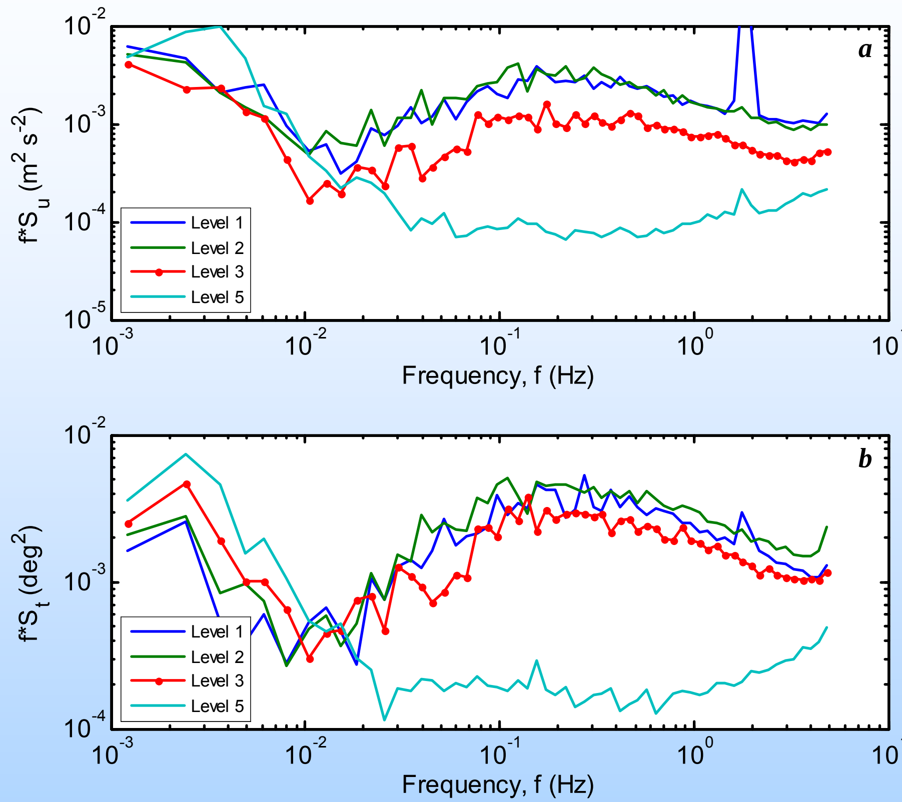

Typical raw spectra of (*a*) the longitudinal wind component and (*b*) the sonic temperature at four levels (level 4 is missing) for very strong stable conditions during 21 December 1997 UTC (1997 YD 355.00). For data presented here the stability parameters at levels 2, 3, and 5 are 3, 10.5, and 116.3 (sensible heat flux is missing for level 1). The bulk Richardson numbers at four levels are Ri_{B1} = 0.0736, Ri_{B2} = 0.0839, Ri_{B3} = 0.1090, and Ri_{B5} = 0.2793

Ekman Surface Layer

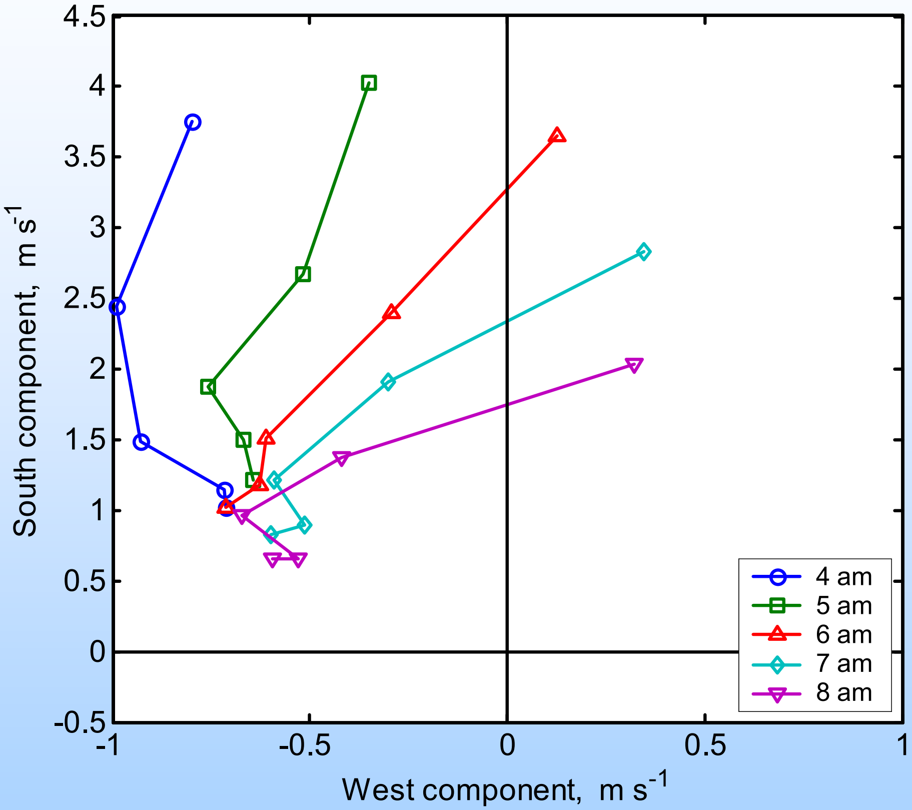

Evolving Ekman-type spirals during the polar day observed during JD 507 (22 May, 1998) for five hours from 12.00 to 16.00 UTC (4:00–8:00 a.m. local time, see the legend). Markers indicate ends of wind vectors at levels 1 to 5 (1.9, 2.7, 4.7, 8.6, and 17.7 m).

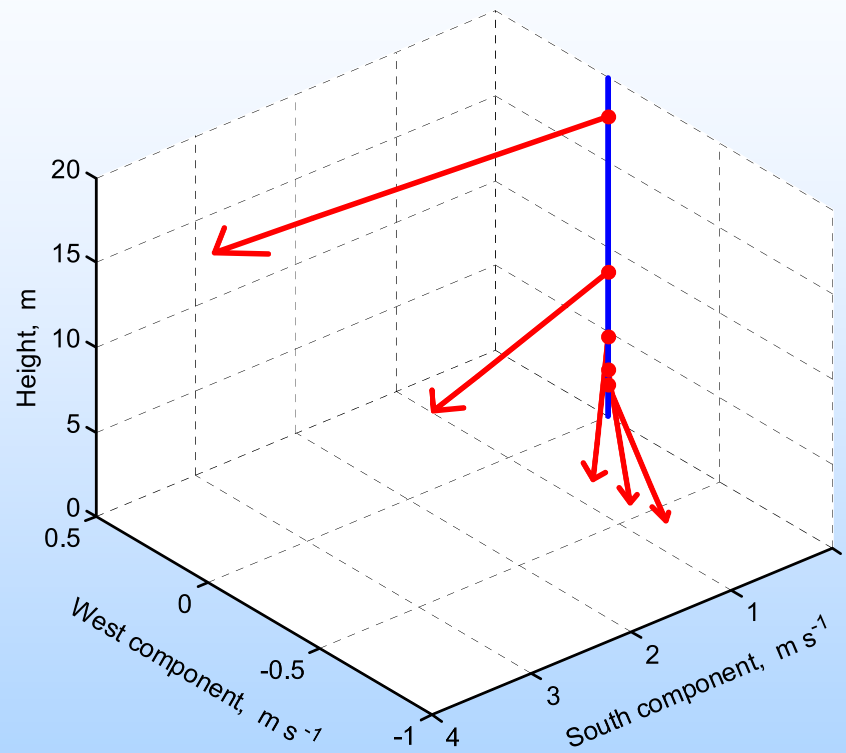

3D view of the Ekman spiral for 14:00 UTC JD 507 (local time 6 a.m.), 22 May 1998

Grachev et al. (2005), *Boundary-Layer Meteorology*, **116**(2), 201-235.

Basic M-O Similarity Equations for Surface Flux

Surface stress:

$$\tau = -\rho\overline{uw} \equiv \rho u_*^2$$

Sensible and latent heat fluxes:

$$H_s = \rho c_p \overline{wt} \equiv -\rho c_p u_* t_* ,$$

$$H_L = \rho L_v \overline{wq} \equiv -\rho L_v u_* q_* .$$

Modeling - basic equations

$$\tau = \rho C_{Dr} S^2$$

$$H_s = \rho c_p C_{Hr} S(\Theta_s - \Theta_r)$$

$$H_L = \rho L_v C_{Er} S(Q_s - Q_r)$$

$$C_{Dr} = c_{Dr}^2 = \left[\frac{k}{\ln(r/z_0) - \psi_m(r/L)}\right]^2$$

$$C_{Hr} = c_{Dr} c_{Hr} = \left[\frac{k}{\ln(r/z_0) - \psi_m(r/L)}\right]\left[\frac{k}{\ln(r/z_T) - \psi_h(r/L)}\right]$$

$$C_{Er} = c_{Dr} c_{Er} = \left[\frac{k}{\ln(r/z_0) - \psi_m(r/L)}\right]\left[\frac{k}{\ln(r/z_Q) - \psi_h(r/L)}\right]$$

z_0 - surface roughness for momentum
z_T - surface roughness for temperature
z_Q - surface roughness for moisture
S - surface layer wind speed
r - reference height (sometimes called z)
L - Monin-Obuhkov length
r/L (z/L) - M-O stability parameter

Improve stability correction function in surface layer parameterizations

$$\varphi_{m\ \mathrm{SHEBA}} = 1 + \frac{a_m \zeta (1+\zeta)^{1/3}}{1 + b_m \zeta} \equiv 1 + \frac{6.5\zeta(1+\zeta)^{1/3}}{1.3+\zeta},$$

$$\varphi_{h\ \mathrm{SHEBA}} = 1 + \frac{a_h \zeta + b_h \zeta^2}{1 + c_h \zeta + \zeta^2} \equiv 1 + \frac{5\zeta + 5\zeta^2}{1 + 3\zeta + \zeta^2},$$

where $a_m \equiv \beta_m = 5$, $b_m = a_m/6.5$, $a_h \equiv \beta_h = 5$, $b_h = 5$, and $c_h = 3$.

Surface stability parameter
$\zeta = z_n/L_1$

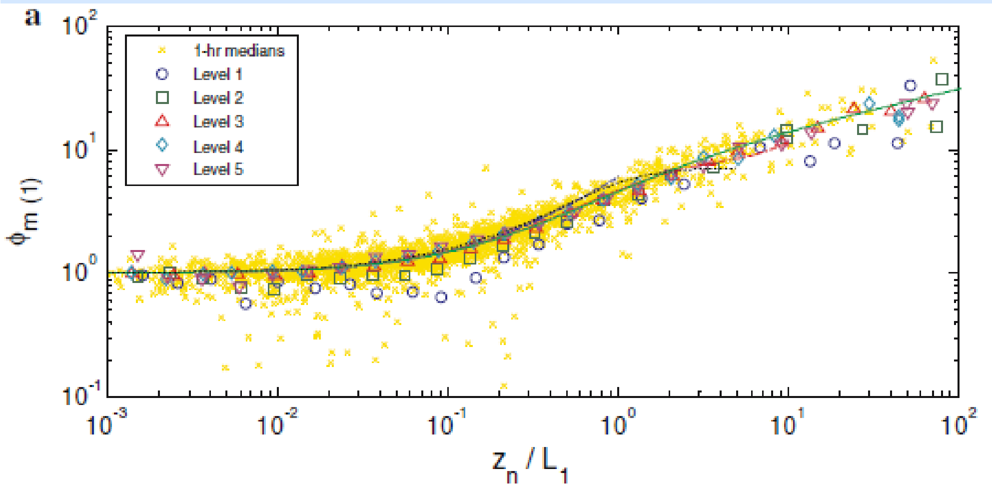

Grachev et al. (2007), *Boundary-Layer Meteorology*, **124**(3), 315 - 333.

New stability correction functions match SHEBA data best for z/L > 10

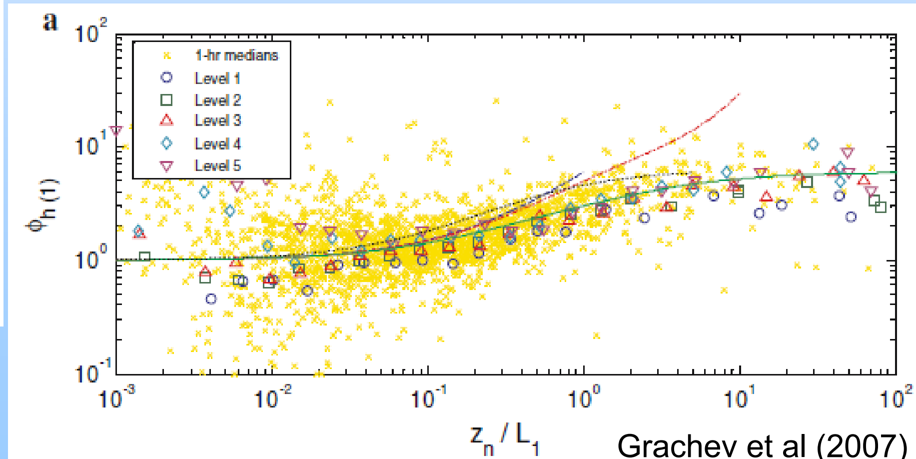

Grachev et al (2007)

Hs/U vs Δθ

- SHEBA Observations (black dots, Nov 1997 – Sep 1998)
- Model/parameterization output – colored dots
- Slope proportional to C_H

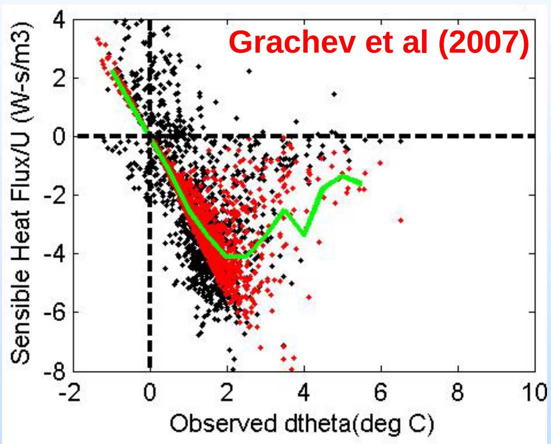

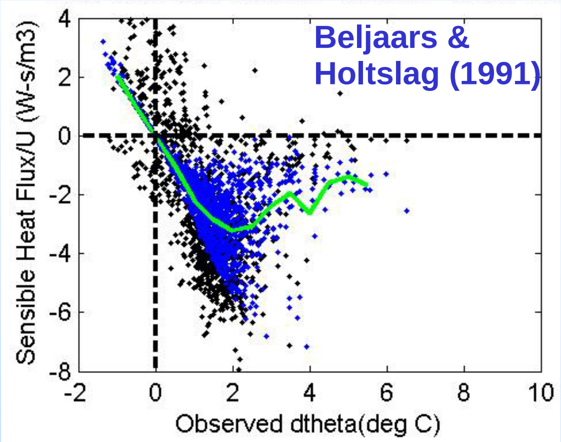

1) Grachev et al (2007) and Beljaars and Holtslag (1991) stability schemes allow for decrease of turbulence to dominate over increased ΔT for very stable conditions

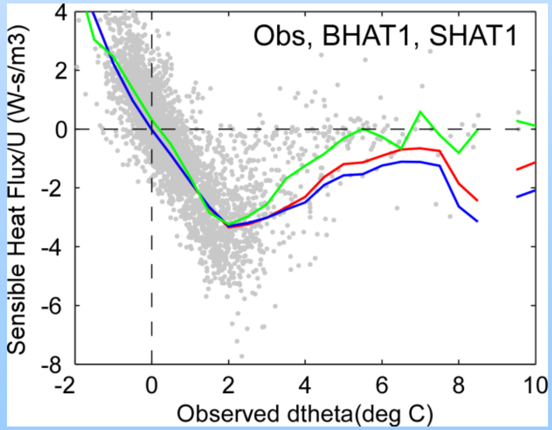

H_s/U as a function of the vertical potential temperature gradient for the observed SHEBA data points (grey dots). The curves are bin-averaged curves for the observed SHEBA data (green), the Beljaars and Holtslag (1991) parameterization (blue), and SHEBA parameterization (Grachev *et al* 2007) (red). Both schemes are able to suppress turbulent fluxes during very stable conditions. Results also indicate that using the Grachev et al stability functions provide a clear advantage over the BH91 functions for times with greater stability.

Enhanced Summertime Roughness

Meltpond and lead edges enhance roughness and drag (C_D)
- increases z_0, C_H and C_E, and thus H_s and H_l for summer and MIZ

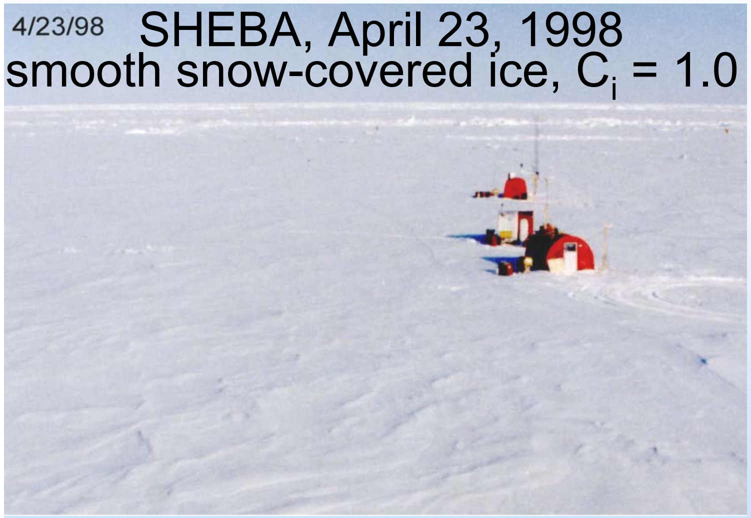

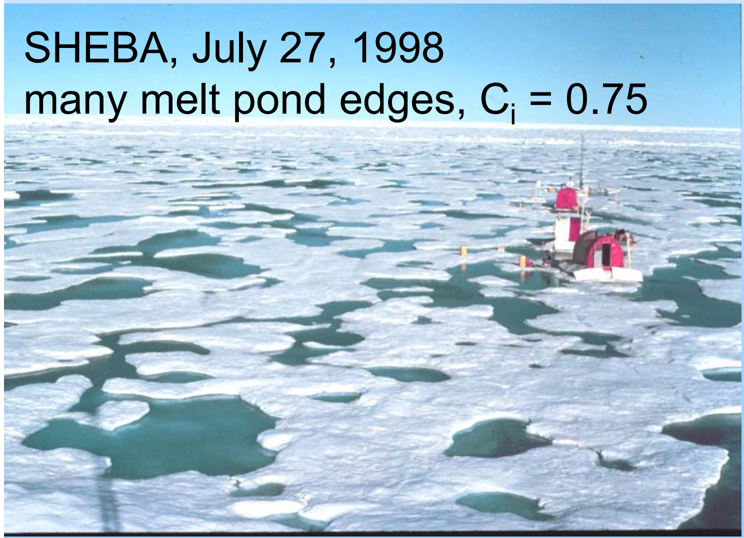

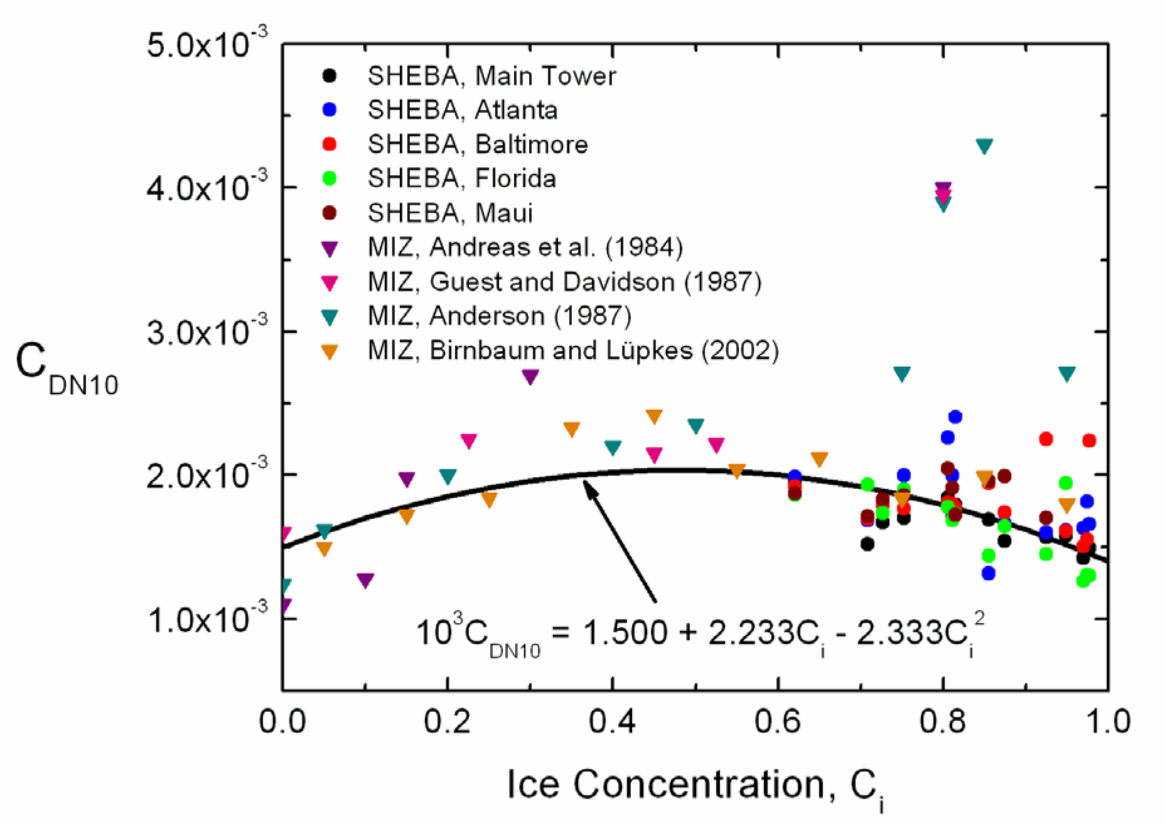

Andreas, E. L, T. W. Horst, A. A. Grachev, P. O. G. Persson, C. W. Fairall, P. S. Guest, and R. E. Jordan, 2010: Parameterising turbulent exchange over summer sea ice and the marginal ice zone. *Quart. J. Roy. Meteor. Soc.*, Accepted.

Sea-Ice Surface Flux Scheme Based on SHEBA Data

(Andreas et al 2010)

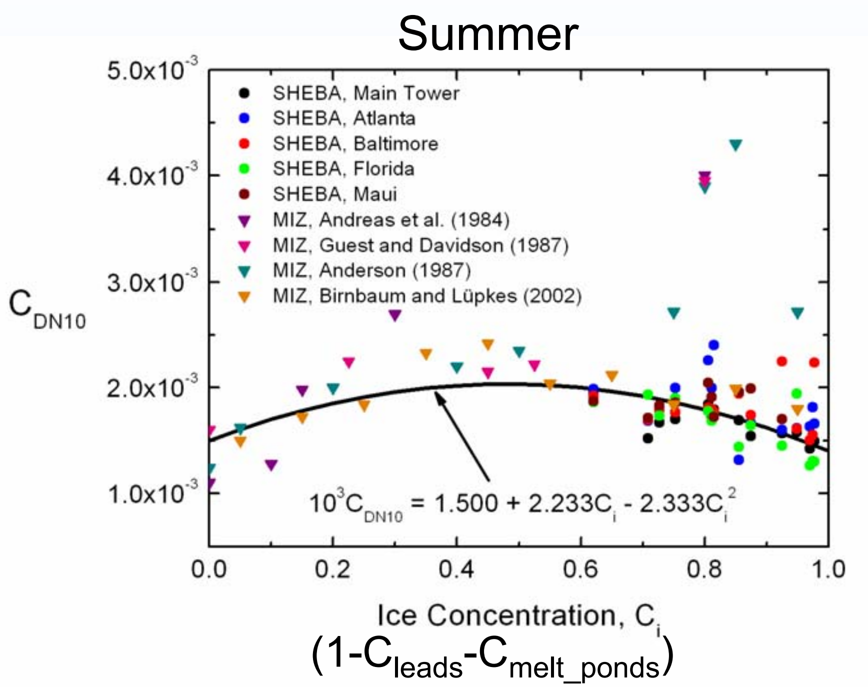

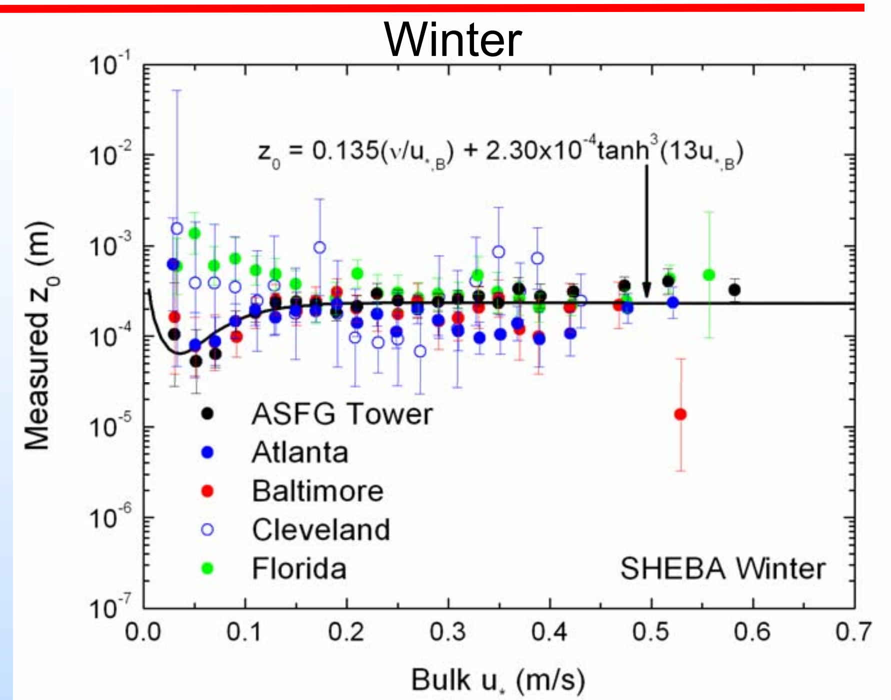

Parameterization Equations

$$\tau = -\rho\overline{uw} \equiv \rho u_*^2 = \rho C_{Dr} S_r^2$$

$$H_s = \rho c_p \overline{w\theta} = \rho c_p C_{Hr} S_r (\Theta_s - \Theta_r)$$

$$H_L = \rho L_v \overline{wq} = \rho L_v C_{Er} S_r (Q_s - Q_r)$$

$$C_{Dr} = \frac{k^2}{\left[\ln(r/z_0) - \psi_m(r/L)\right]^2}$$

$$C_{Hr} = \frac{k C_{Dr}^{1/2}}{\left[\ln(r/z_T) - \psi_h(r/L)\right]}$$

$$C_{Er} = \frac{k C_{Dr}^{1/2}}{\left[\ln(r/z_Q) - \psi_h(r/L)\right]}$$

$$L = -\frac{\overline{\Theta}_v}{kg}\left(\frac{u_*^3}{\overline{w\theta_v}}\right)$$

$$S_r = \left(U_r^2 + \beta_g^2 w_*^2\right)^{1/2}$$

$$w_* = u_*\left(-\frac{z_i}{kL}\right)^{1/3}$$

$$S_r = U_r + 0.5\,\mathrm{sech}(U_r)$$

$$C_{DN10} = \frac{k^2}{\left[\ln(10/z_0)\right]^2}$$

$$C_{HN10} = \frac{k^2}{\left[\ln(10/z_0)\right]\left[\ln(10/z_T)\right]}$$

$$C_{EN10} = \frac{k^2}{\left[\ln(10/z_0)\right]\left[\ln(10/z_Q)\right]}$$

$$z_0 = 0.135\frac{\nu}{u_{*,B}} + 2.30\times10^{-4}\tanh^3(13u_{*,B})$$

$$\ln(z_s/z_0) = b_0 + b_1 \ln R_* + b_2 (\ln R_*)^2$$

$$10^3 C_{DN10} = 1.500 + 2.233 C_i - 2.333 C_i^2$$

ψ_m and ψ_h, given in Paulson (1970) (unstable) and Grachev et al. (2007) (stable)

FORTRAN code available from:
eandreas@nwra.com

*Workshop * Surface Fluxes: Challenges for High Latitudes * NCAR Boulder Colorado * March 17-19, 2010*

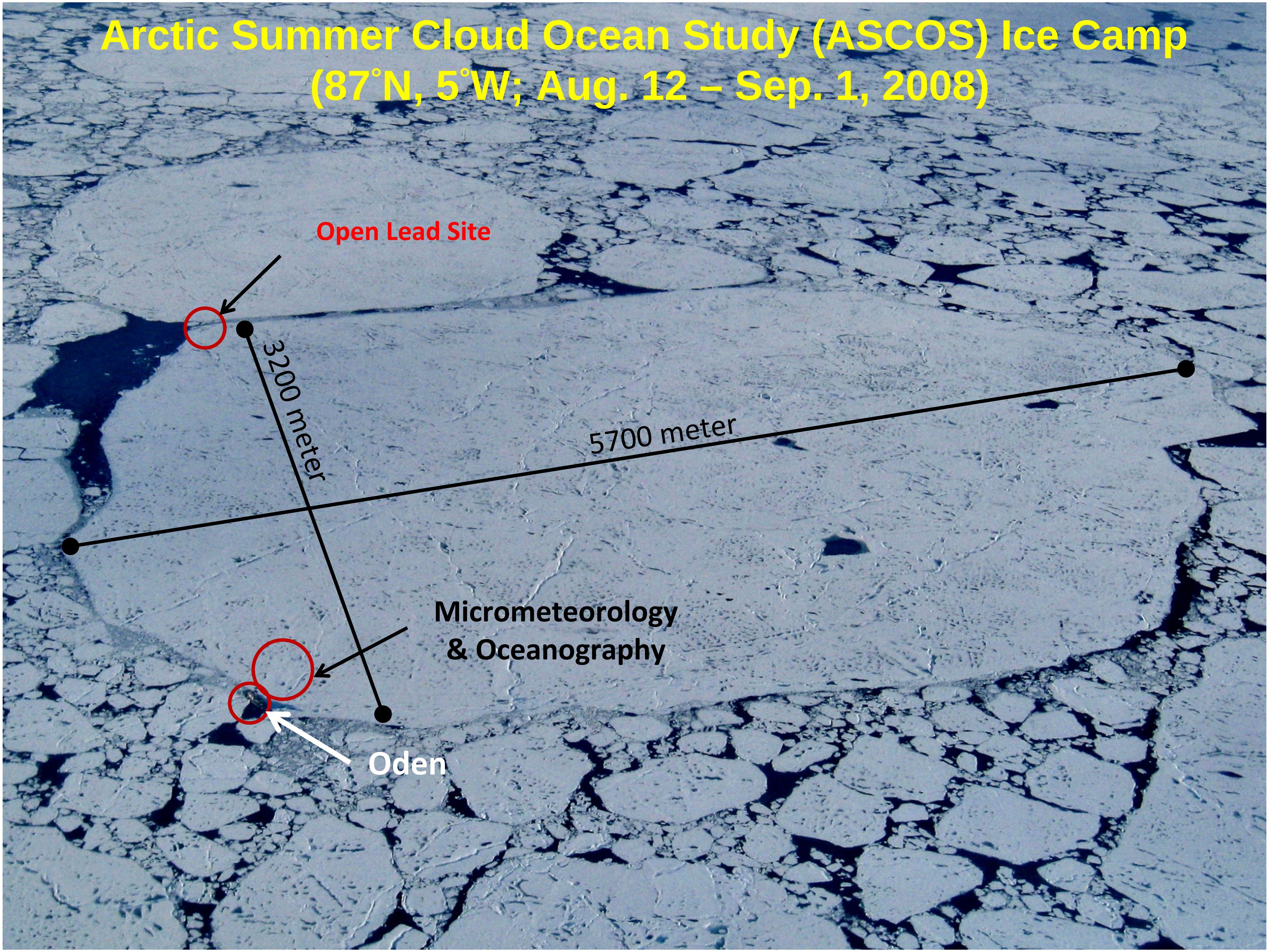
Arctic Summer Cloud Ocean Study (ASCOS) Ice Camp
(87°N, 5°W; Aug. 12 – Sep. 1, 2008)
Open Lead Site
3200 meter
5700 meter
Micrometeorology
& Oceanography
Oden


Swedish Icebreaker Oden on Site at 87.4N,5.8W, Aug. 15, 2008, 0930 UTC
CIRES/NOAA/CET Remote Sensors
Other instrumentation
60 GHz Scanning Radiometer
Air Chemistry sampling
(U. of Stockholm, & others)
449 MHz Wind Profiler
Lidar (Italian)
S-band Cloud and
Precipitation Radar
MAERI (U. of Miami)
4X Daily Rawinsondes
(U of Stockholm)
Dual-channel Microwave Radiometer
Millimeter Wavelength Cloud Radar (MMCR)
Taken from NASA DC-8 Research Aircraft. Photo by: Ron Wilcox

ASCOS Turbulent and Radiative Fluxes

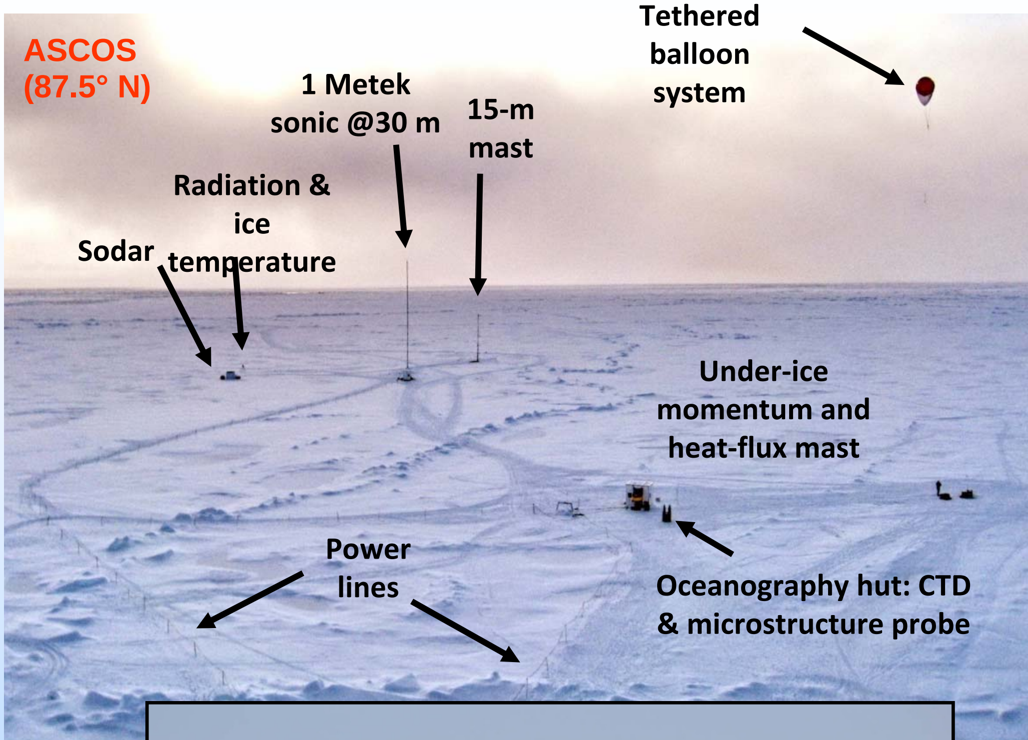

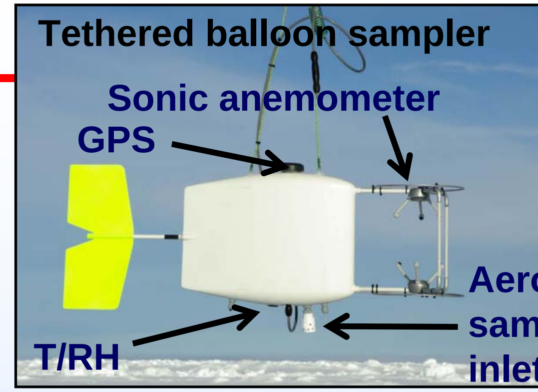

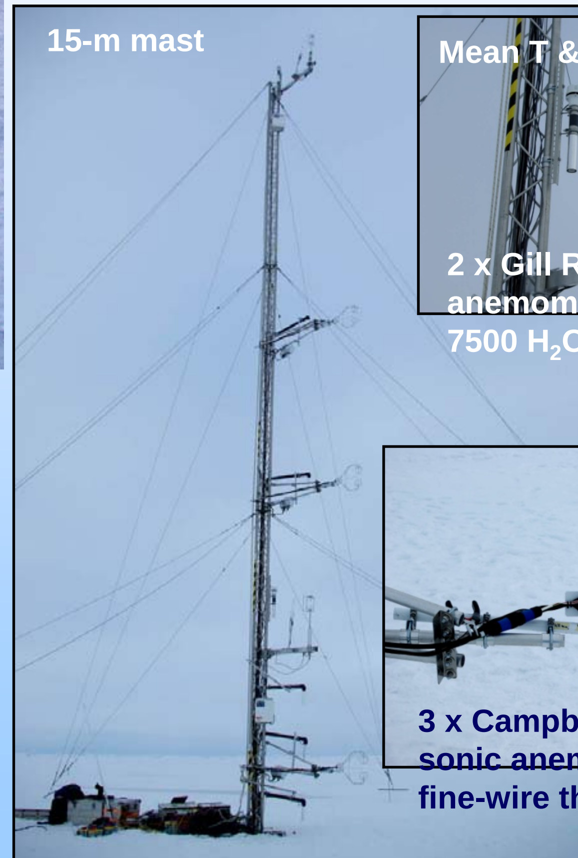

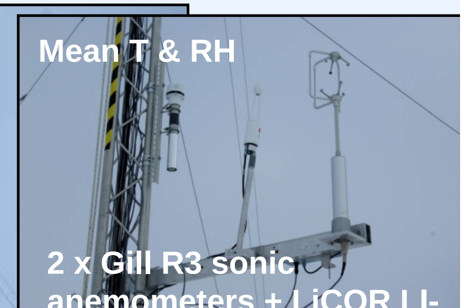

ASCOS Roughness Lengths

(Birch 2010)

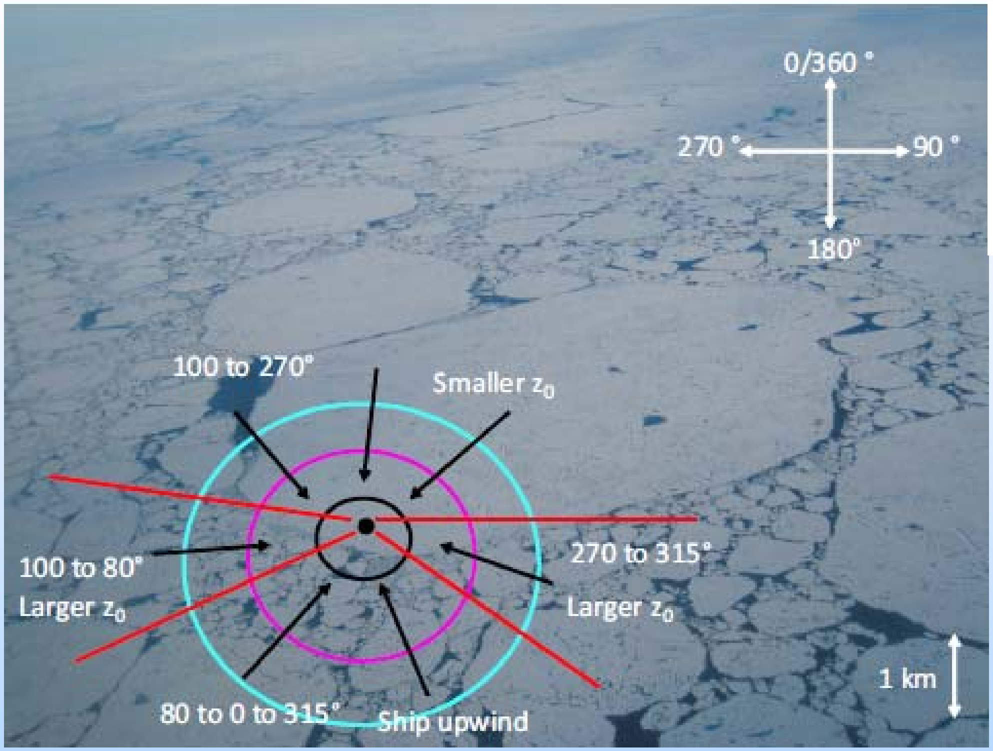

Figure 5.23: z_0 measurements in terms of the local floe. Arrows point in direction wind is blowing. The cyan, magenta and black circles represent the approximate limit of the 90 % flux source area for the instruments at 30.60 m, 15.40 m and 8.19 m respectively.

Table 5.3: Values of C_{DN10} and z_0 measured at the open lead site.

Sector	Ice type	C_{DN10}	z_0
A	Open lead/ice edge	2.22×10^{-3}	5.7×10^{-3}
B	Rough ice	2.78×10^{-3}	3.2×10^{-3}
C	Ice floe	1.26×10^{-3}	6.1×10^{-4}
D	Ice floe	1.53×10^{-3}	9.1×10^{-4}
E	Fairly rough ice	2.74×10^{-3}	4.4×10^{-3}
F	Open lead/ice edge	1.63×10^{-3}	1.3×10^{-3}

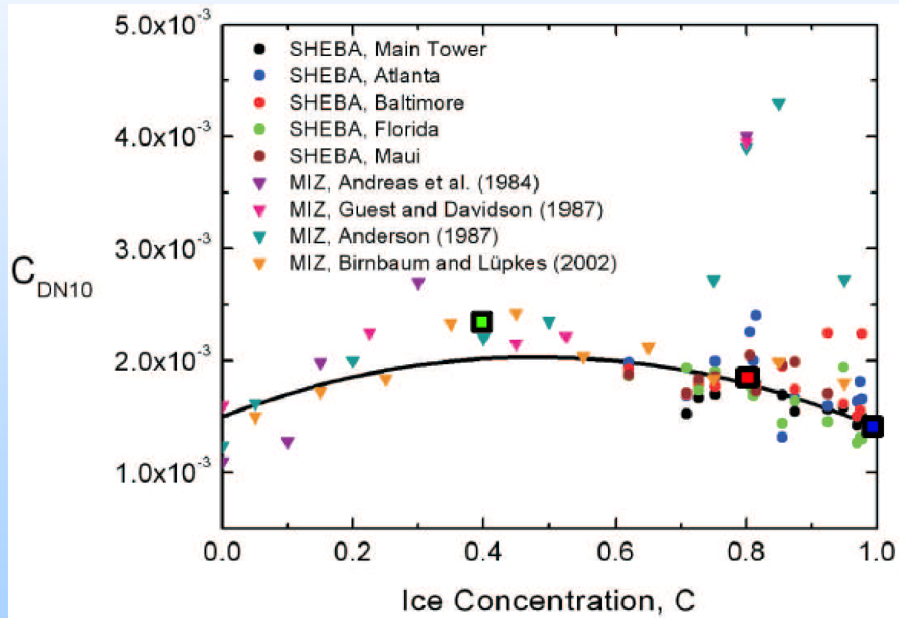

Figure 5.27: Summertime parameterisation for C_{DN10} over sea ice. The black line is a quadratic fit (Equation 5.23) to observations from the SHEBA experiment, observations in the Antarctic marginal ice zone by Andreas *et al.* (1984) and observations in the Arctic marginal ice zone by Guest & Davidson (1987), Anderson (1987) and Birnbaum & Lüpkes (2002). Original plot taken from Andreas *et al.* (2009). Values of C_{DN10} calculated from ASCOS observations have been added to the plot; rough ice at the mast site (red square), rough ice at the open lead site (green square) and smooth ice from the open lead and mast sites (blue square).

Fall Transition Regimes During ASCOS

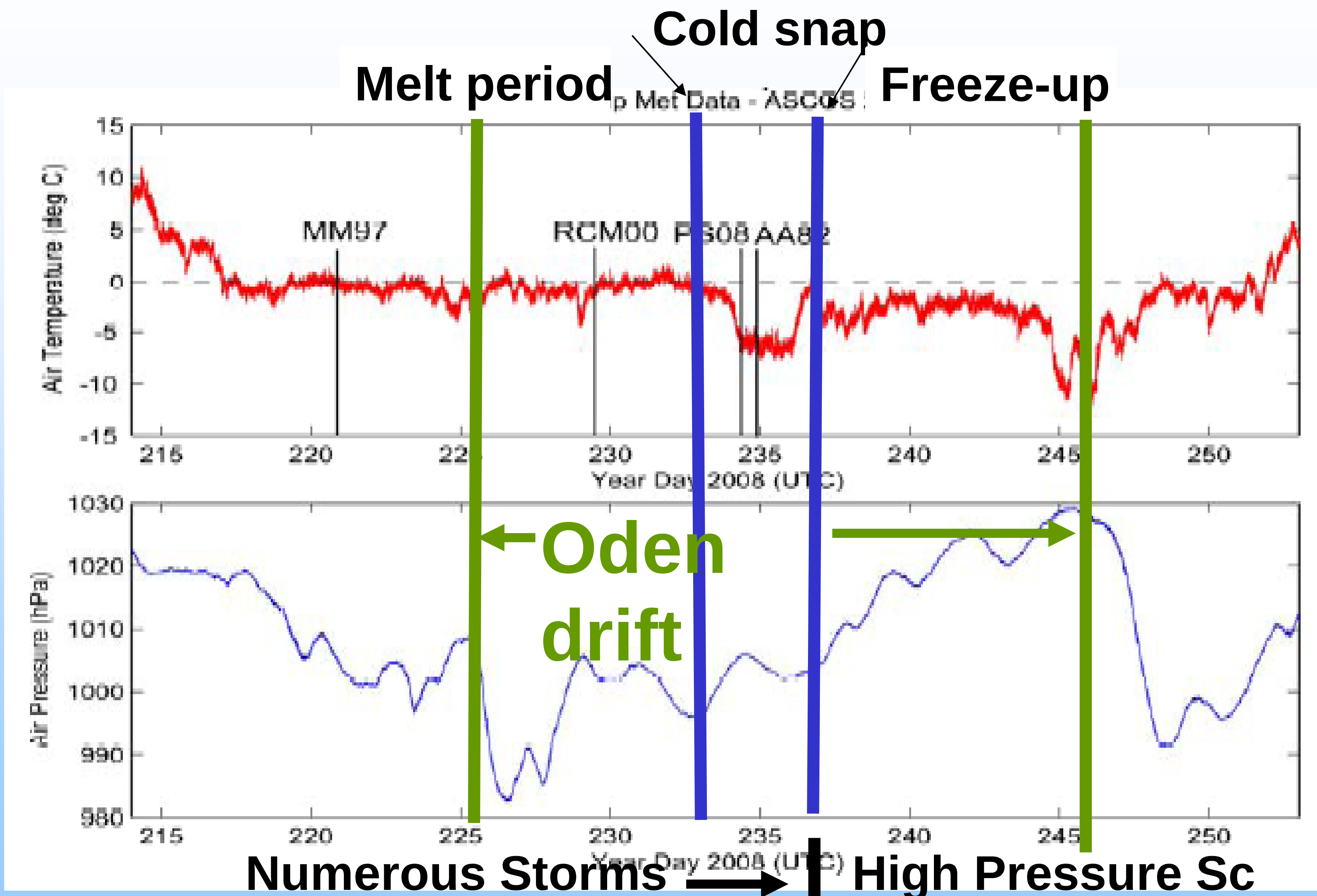

Sample Days – Cloud radar perspective

Melt/Storm Period (Aug. 15-16; YD228-229)

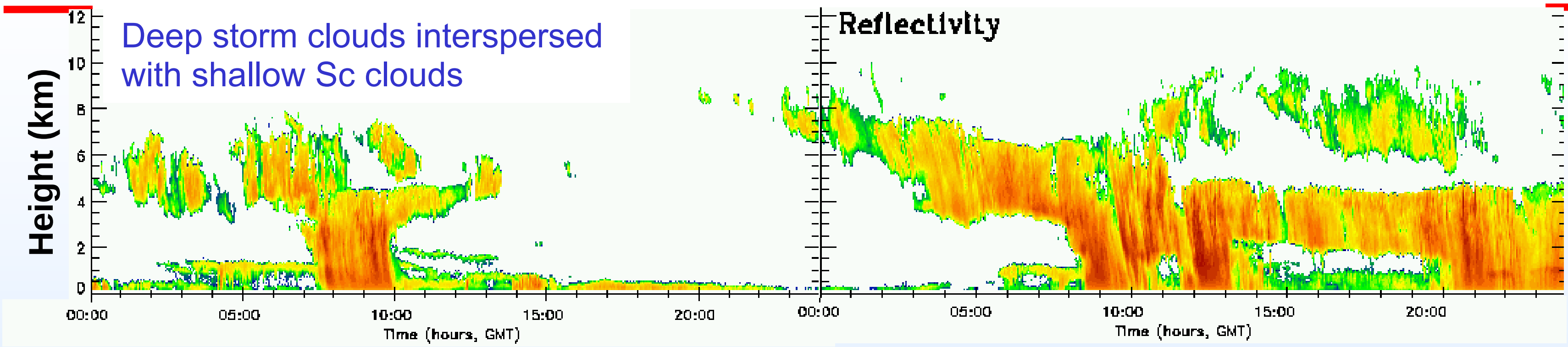

Sample Days – Cloud radar perspective

Melt/Storm Period (Aug. 15-16; YD228-229)

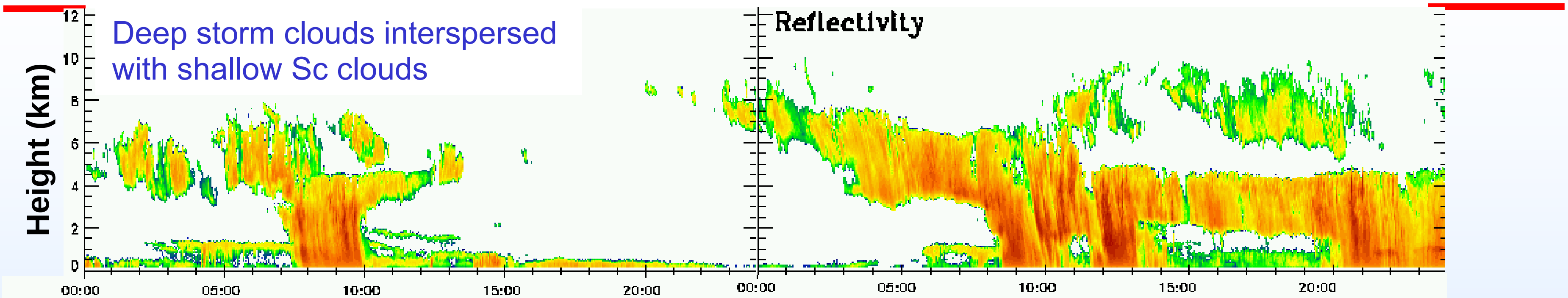

Cold Snap Period (Aug. 21-22; YD234-235)

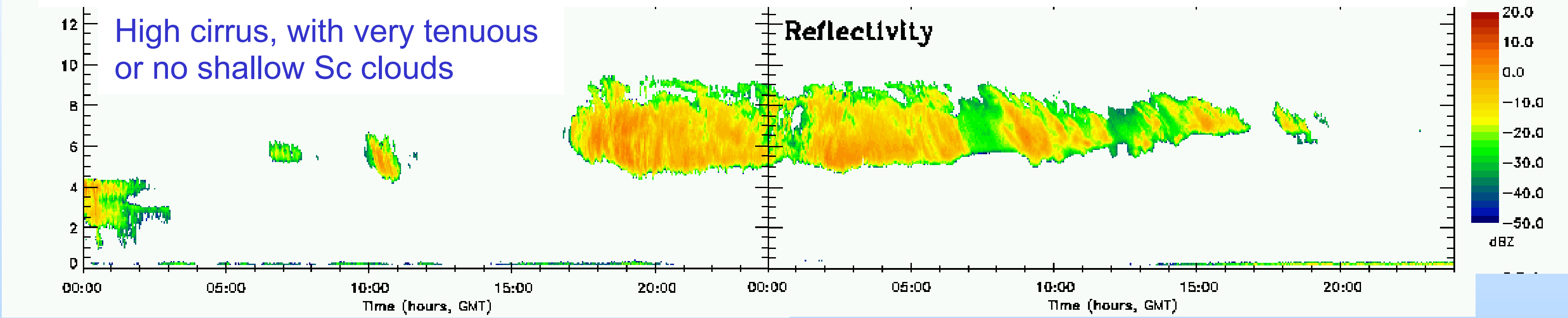

Sample Days – Cloud radar perspective

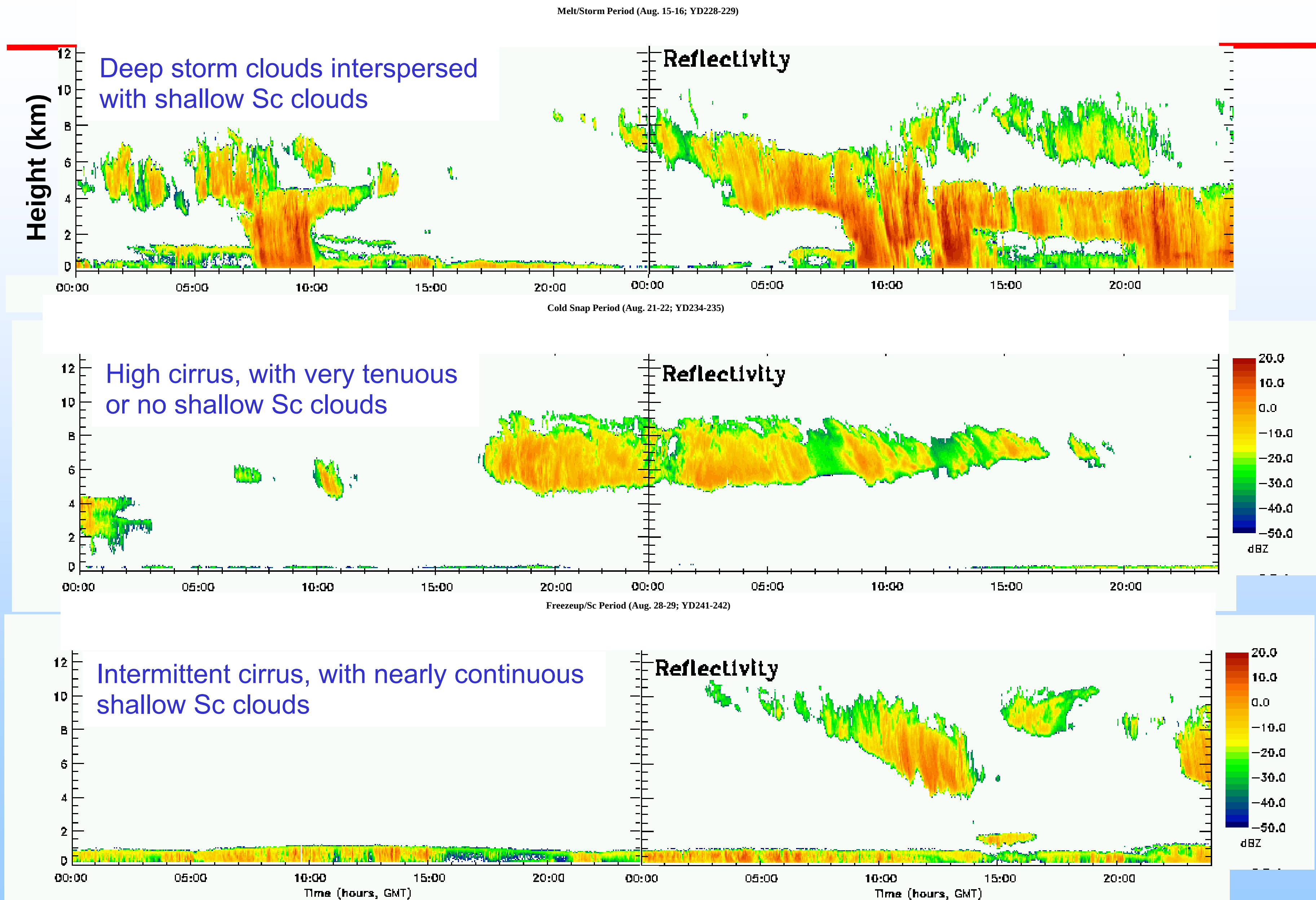

Turbulent Flux Data -ASCOS

Median H_s and τ from 6 tower levels (0.94, 4.04, 5.27, 8.19, 15.40, 30.60 m)
- 5-point running means of 10-min average data

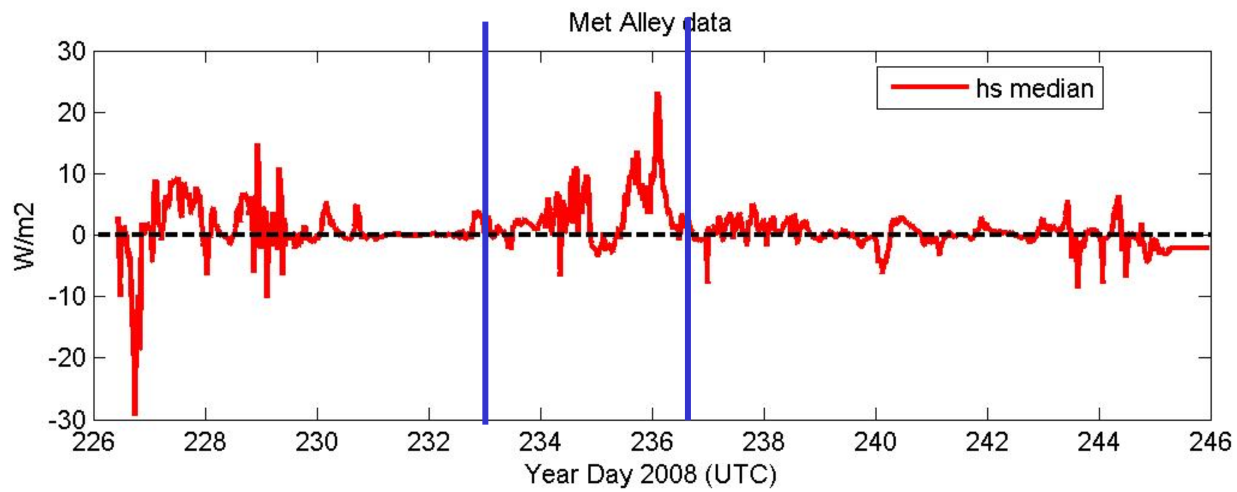

H_s active during storms and cold snap, quite small during Sc regime

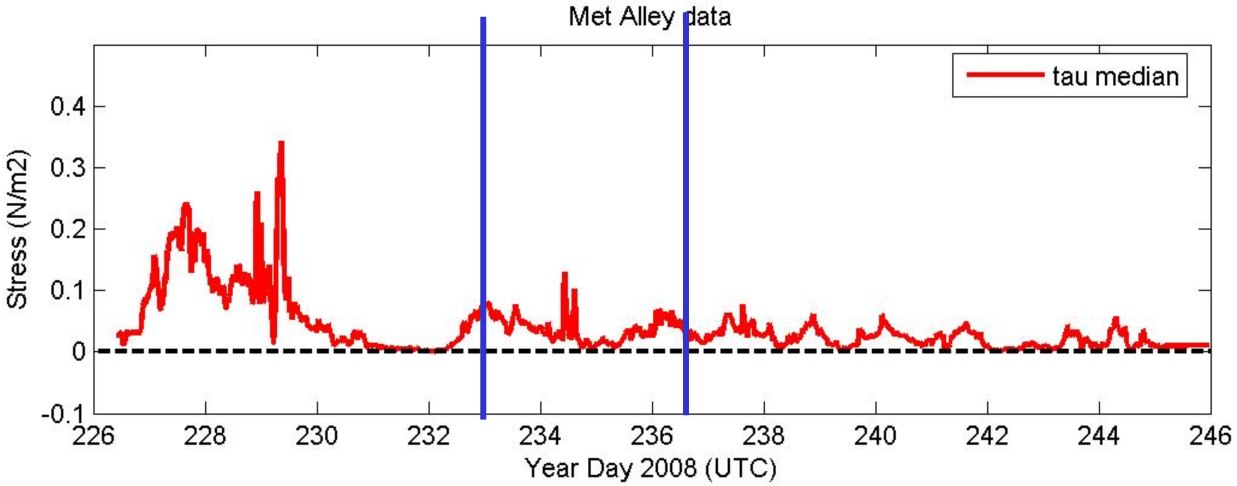

τ significant during storms, quite small during Sc regime

Turbulent Flux Data -ASCOS

H_s and τ estimates from Marine-Atmospheric Emitted Radiance Interferometer (M-AERI)

- T_s (downward look) and T_a (horizontal look), ship-based U and q
- COARE bulk scheme, Grachev et al (2007) stability correction, Andreas (1987) z_0

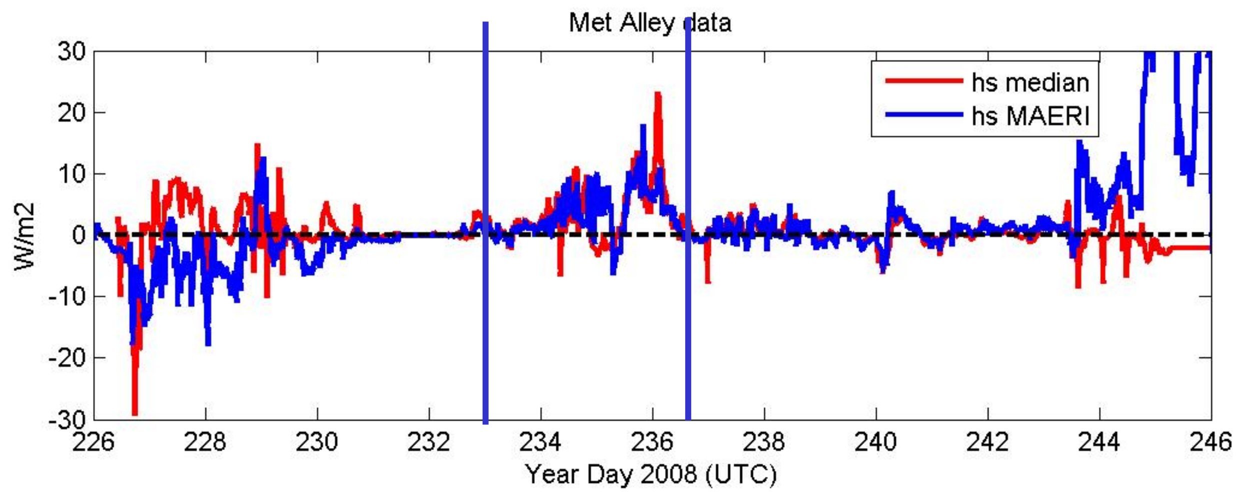

Good match except when ship moves and lead sampled by M-AERI

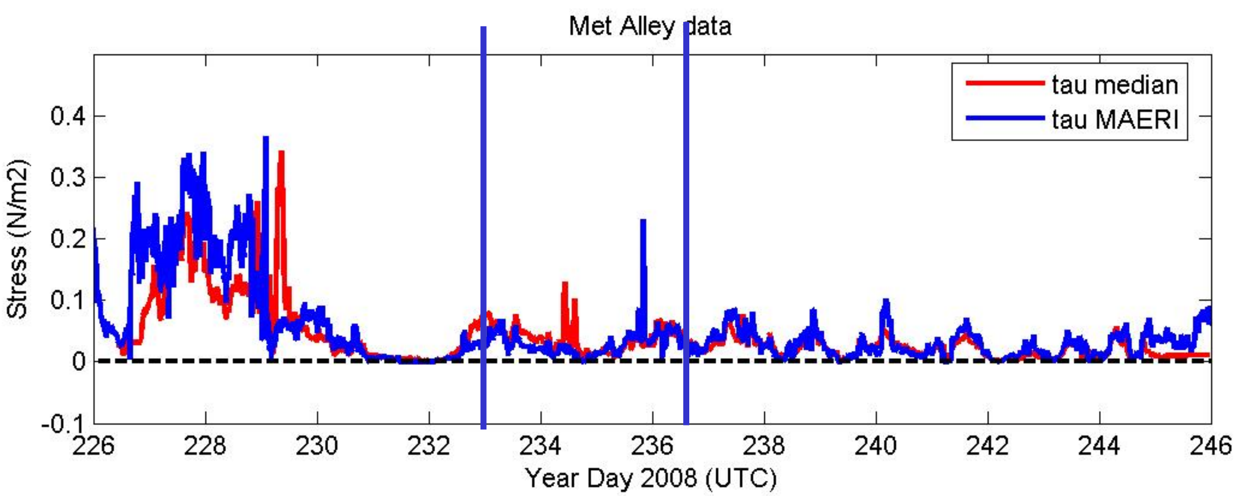

Good match

Turbulent Flux Data -ASCOS

H_l estimate from M-AERI bulk technique

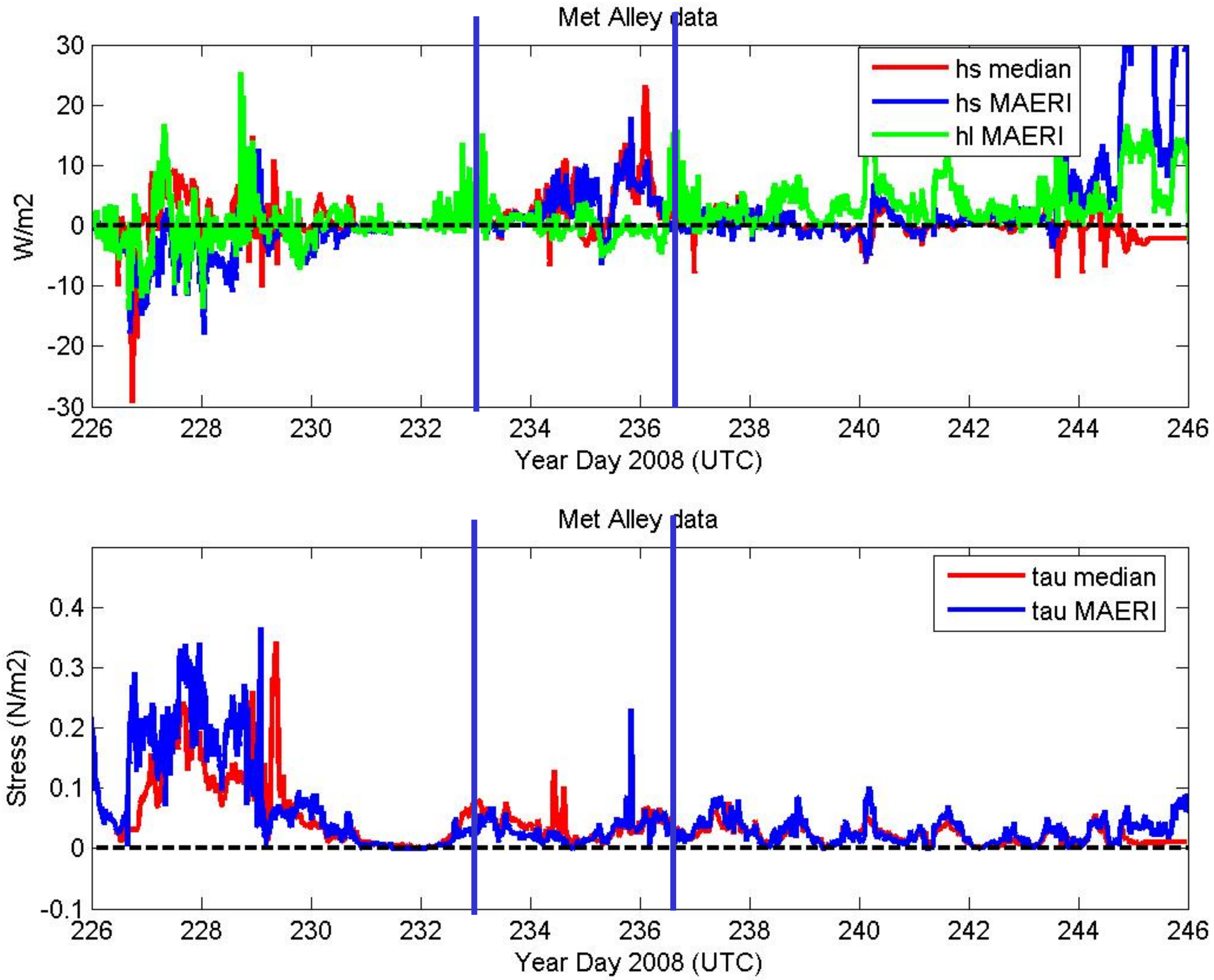

H_l as large or larger than H_s, esp. during Sc period. Sometimes out of phase with H_s.

Daily Surface Energy Budget – end of summer melt

Melting during storm period ($F_{net} > 0$)

During Sc period, T_s near freezing point of seawater and no surface energy flux ($F_{net} \approx 0$)

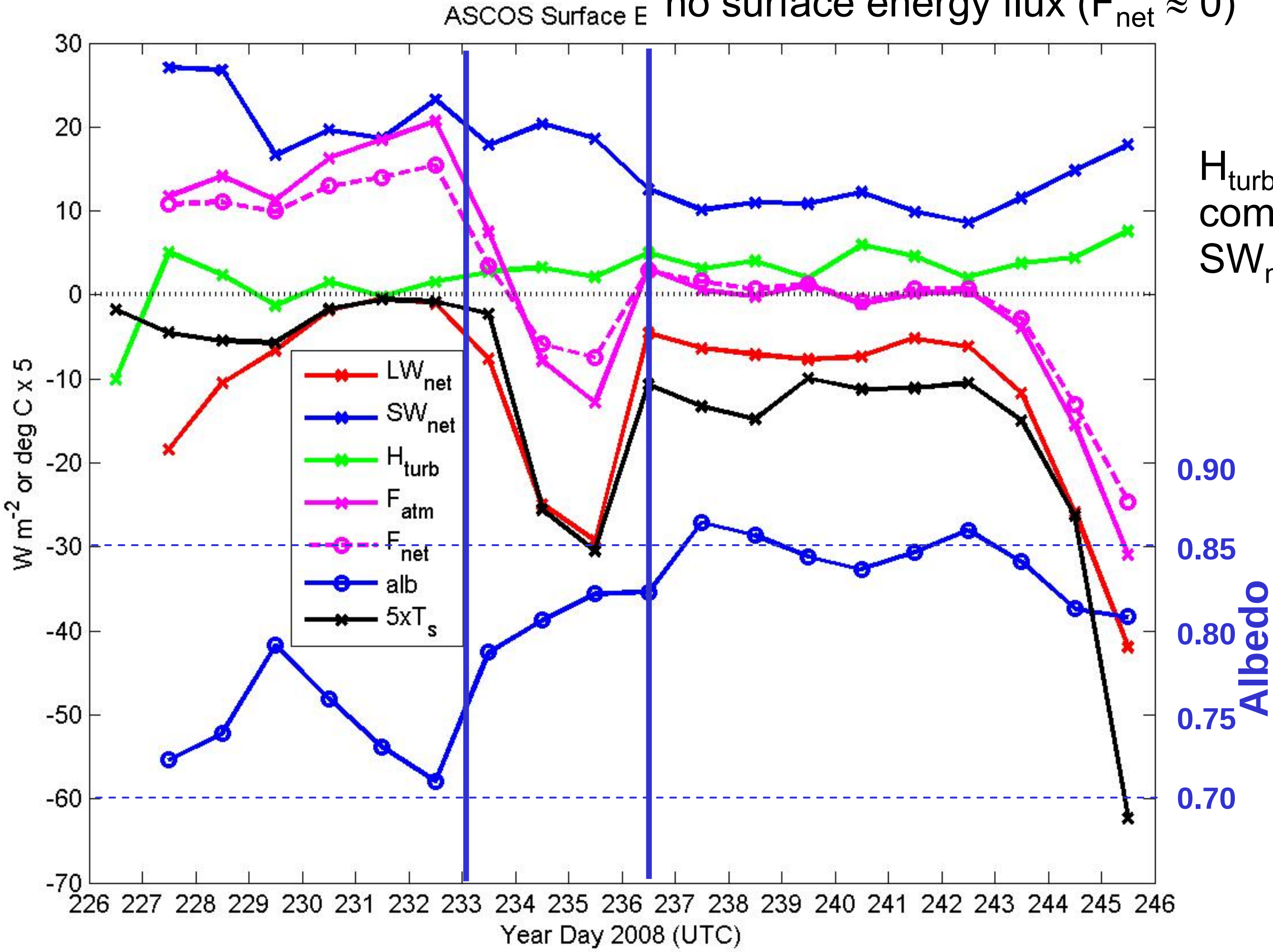

H_{turb} significant compared to SW_{net}+ LW_{net}

α increased from 0.72-0.83 -significant reduction of SW_{net}

Questions?